Journal of Medicinal Chemistry

Article

Cite This: J. Med. Chem. 2018, 61, 2266−2277

pubs.acs.org/jmc

A Systematic Exploration of Macrocyclization in Apelin-13: Impact on Binding, Signaling, Stability, and Cardiovascular Effects

Kien Trân,[†,∥] Alexandre Murza,[†,∥] Xavier Sainsily,[†,∥] David Coquerel,[‡,∥] Jérôme Côté,[†,∥] Karine Belleville,[†,∥] Lounès Haroune,[†,∥] Jean-Michel Longpré,[†,∥] Robert Dumaine,[†,∥] Dany Salvail,[§] Olivier Lesur,[‡,∥] Mannix Auger-Messier,[‡] Philippe Sarret,[†,∥,⊥] and Éric Marsault*[,†,∥,⊥]

[†]Département de Pharmacologie-Physiologie, Faculté de Médecine et des Sciences de la Santé, Université de Sherbrooke, Sherbrooke J1H 5N4, Québec, Canada

[‡]Département de Médecine, Faculté de Médecine et des Sciences de la Santé, Université de Sherbrooke, Sherbrooke J1H 5N4, Québec, Canada

[§]IPS Thérapeutique Inc., Sherbrooke J1G 5J6, Québec, Canada

[∥]Institut de Pharmacologie de Sherbrooke, Sherbrooke J1H 5N4, Québec Canada

Supporting Information

ABSTRACT: The apelin receptor generates increasing interest as a potential target across several cardiovascular indications. However, the short half-life of its cognate ligands, the apelin peptides, is a limiting factor for pharmacological use. In this study, we systematically explored each position of apelin-13 to find the best position to cyclize the peptide, with the goal to improve its stability while optimizing its binding affinity and signaling profile. Macrocyclic analogues showed a remarkably higher stability in rat plasma (half-life >3 h versus 24 min for Pyr-apelin-13), accompanied by improved affinity (analogue **15**, K_i 0.15 nM and $t_{1/2}$ 6.8 h). Several compounds displayed higher inotropic effects ex vivo in the Langendorff isolated heart model in rats (analogues **13** and **15**, maximum response at 0.003 nM versus 0.03 nM of apelin-13). In conclusion, this study provides stable and active compounds to better characterize the pharmacology of the apelinergic system.

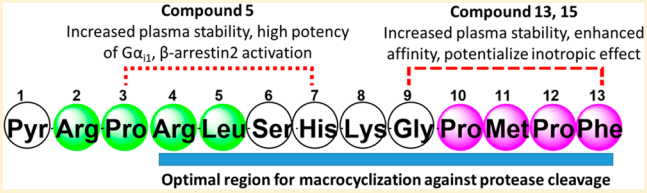

INTRODUCTION

Apelin is the endogenous ligand of the apelin receptor (also known as APJ or angiotensin receptor-like 1), which belongs to the G protein-coupled receptor (GPCR) superfamily.[1] In humans, the APLN gene on chromosome X encodes for the 77-amino-acid precursor, preproapelin,[2,3] which is cleaved to generate several isoforms: apelin-36, apelin-17, apelin-13, and apelin-13(1-12) (collectively called hereafter the apelins).[2,4,5] Among them, the pyroglutamate form of apelin-13 (Pyr-apelin-13, referred below as apelin-13) is the most abundant in human plasma.[6] Structurally, apelin-13 is composed of two distant pharmacophoric regions: the *N*-terminal RPRL (Arg^2-Pro^3-Arg^4-Leu^5), essential for binding affinity,[7,8] and the C-terminal PMPF (Pro^{10}-Met^{11}-Pro^{12}-Phe^{13}), important for both binding affinity and signaling.[7,9] Binding of the apelins to the APJ receptor triggers several intracellular signaling pathways, mediated by the $G\alpha_{i/o}$, $G\alpha_{13}$, and possibly the $G\alpha_q$ proteins, subsequently leading to the recruitment of several signal transduction cascades such as the activation of PLC/PKCε,[10−12] AMP-activated protein kinase (AMPK)/eNOS,[13−15] as well as the regulation of ERK1/2 phosphorylation and PI3K/Akt/p70S6 kinase signaling.[16,17] Another APJ ligand, ELABELA (ELA, also known as Toddler, or Apela), was reported in 2013 to exhibit the same affinity for the receptor and to exert similar signaling profiles as the apelins.[18,19] Importantly, both ligands are critical regulators of cardiovascular development and function.[9,20−22]

Existing knowledge collectively makes the APJ receptor a compelling target for the treatment of cardiovascular diseases.[23] Physiologically, apelins stimulate cardiac contractility while decreasing peripheral resistance and promoting angiogenesis.[23,24] A decrease in APJ receptor density in the left ventricle has also been observed in dilated cardiomyopathy and cardiac ischemia patients.[25] Although reports on the levels of apelins and ELA in diverse pathologies may be contradictory,[26] apelin-13 treatment has consistently shown a positive impact on cardiac contractility and lowering of the mean arterial blood pressure (MABP) in heart failure patients.[27,28] Investigator trials on pulmonary arterial hypertension (PAH) patients confirmed this therapeutic potential, wherein apelin infusions improved cardiac output and lowered pulmonary vascular resistance.[29] Those beneficial effects of apelin-13 and ELA were demonstrated in many animal models.[30−32] Likewise, our group recently reported their benefits on cardiac and renal functions as well as survival in a systemic inflammation model of sepsis and septic shock.[33,34]

Received: September 13, 2017
Published: February 20, 2018

DOI: 10.1021/acs.jmedchem.7b01353
J. Med. Chem. 2018, 61, 2266−2277

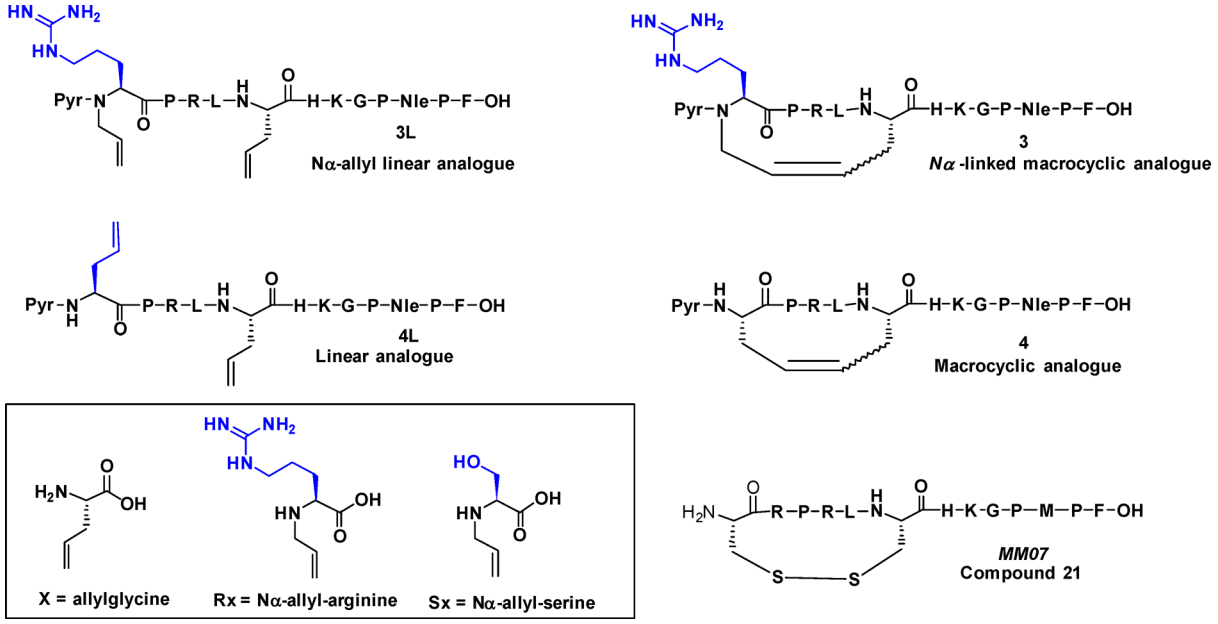

Figure 1. Examples of macrocycles and linear analogues.

Scheme 1. Synthetic Strategy of Linear and Macrocyclic Peptides on Wang Resin[a]

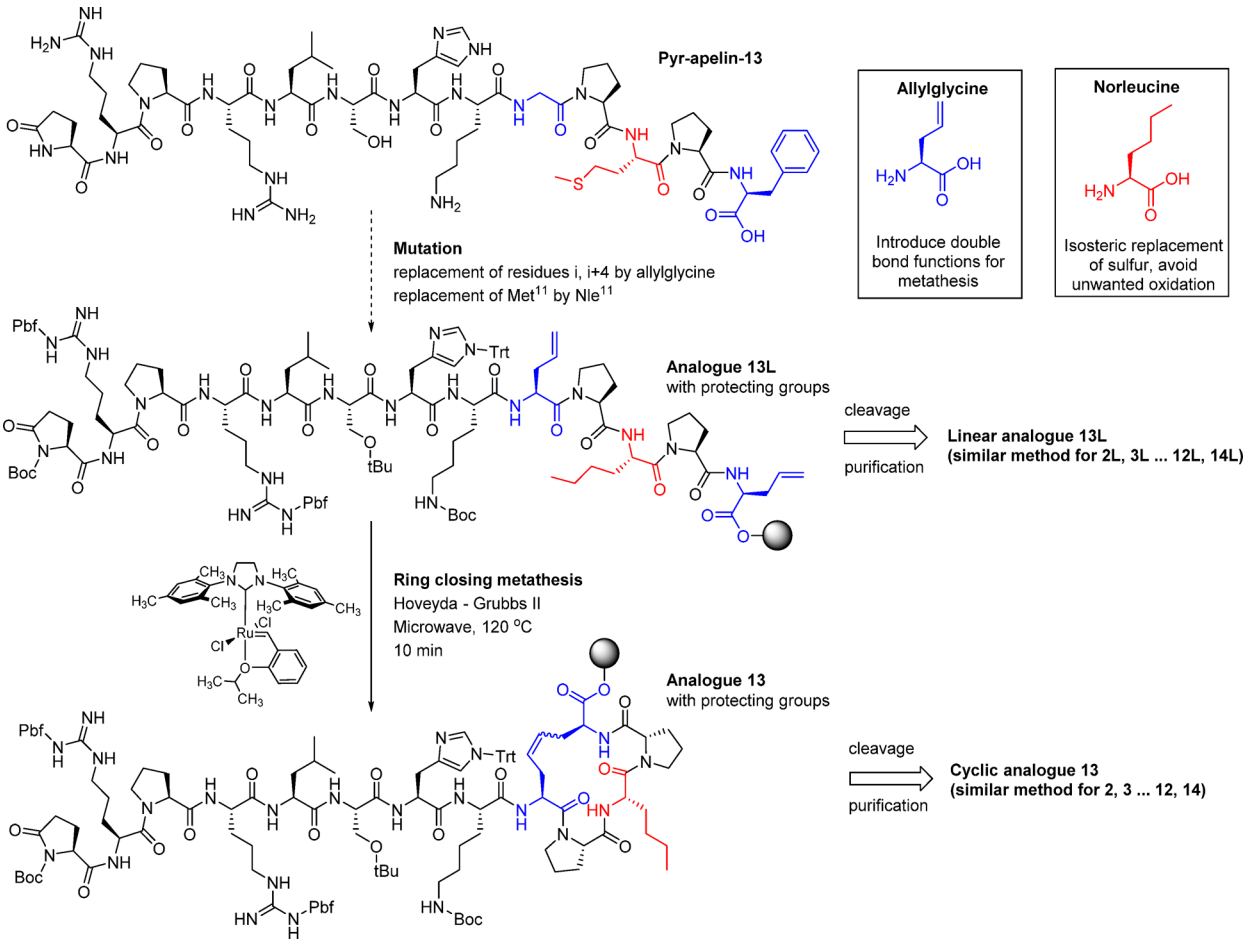

[a]Two residues at *i* and *i*+4 positions of Pyr[1]-apelin-13 were replaced by allylglycine. The product was cleaved to give the linear analogues or cyclized on resin using ring closing metathesis to produce the macrocyclic analogues.

While the therapeutic potential of the apelinergic system is promising, the short half-life of apelin-13 and other apelins remains a limiting factor for their pharmacological use. Indeed, the half-life ($t_{1/2}$) of Pyr-apelin-13 is around 24 min in rat

DOI: 10.1021/acs.jmedchem.7b01353
J. Med. Chem. 2018, 61, 2266−2277

Table 1. Binding Affinity of Pyr[1]-apelin-13 Analogues

no.	linear analogues[a]	K_i binding (nM)[b]	no.	macrocyclic analogues[a]	K_i binding (nM)[b]
Ape13	Pyr-R-P-R-L-S-H-K-G-P-M−P-F	0.7 ± 0.1			
1	Pyr-R-P-R-L-S-H-K-G-P-**Nle**-P-F	0.8 ± 0.2			
2L	**X**-R-P-R-**X**-S-H-K-G-P-**Nle**-P-F	2.5 ± 0.8	**2**	c[**X**-R-P-R-**X**]c-S-H-K-G-P-**Nle**-P-F	5.7 ± 3.5
3L	Pyr-**Rx**-P-R-L-**X**-H-K-G-P-**Nle**-P-F	2.9 ± 1.3	**3**	Pyr-c[**Rx**-P-R-L-**X**]c-H-K-G-P-**Nle**-P-F	4.5 ± 1.4
4L	Pyr-**X**-P-R-L-**X**-H-K-G-P-**Nle**-P-F	523 ± 165	**4**	Pyr-c[**X**-P-R-L-**X**]c-H-K-G-P-**Nle**-P-F	509 ± 146
5L	Pyr-R-**X**-R-L-S-**X**-K-G-P-**Nle**-P-F	1.9 ± 0.2	**5**	Pyr-R-c[**X**-R-L-S-**X**]c-K-G-P-**Nle**-P-F	3.0 ± 0.1
6L	Pyr-R-P-**Rx**-L-S-H-**X**-G-P-**Nle**-P-F	2.7 ± 0.3	**6**	Pyr-R-P-c[**Rx**-L-S-H-**X**]c-G-P-**Nle**-P-F	9.1 ± 1.4
7L	Pyr-R-P-**X**-L-S-H-**X**-G-P-**Nle**-P-F	489 ± 186	**7**	Pyr-R-P-c[**X**-L-S-H-**X**]c-G-P-**Nle**-P-F	6074 ± 1168
8L	Pyr-R-P-R-**X**-S-H-K-**X**-P-**Nle**-P-F	3.9 ± 1.4	**8**	Pyr-R-P-R-c[**X**-S-H-K-**X**]c-P-**Nle**-P-F	41 ± 5
9L	Pyr-R-P-R-L-**Sx**-H-K-G-**X**-**Nle**-P-F	41 ± 4	**9**	Pyr-R-P-R-L-c[**Sx**-H-K-G-**X**]c-**Nle**-P-F	188 ± 84
10L	Pyr-R-P-R-L-**X**-H-K-G-**X**-**Nle**-P-F	194 ± 70	**10**	Pyr-R-P-R-L-c[**X**-H-K-G-**X**]c-**Nle**-P-F	268 ± 125
11L	Pyr-R-P-R-L-S-**X**-K-G-P-**X**-P-F	0.3 ± 0.1	**11**	Pyr-R-P-R-L-S-c[**X**-K-G-P-**X**]c-P-F	1.4 ± 0.4
12L	Pyr-R-P-R-L-S-H-**X**-G-P-**Nle**-**X**-F	2.3 ± 0.2	**12**	Pyr-R-P-R-L-S-H-c[**X**-G-P-**Nle**-**X**]c-F	14 ± 7
13L	Pyr-R-P-R-L-S-H-K-**X**-P-**Nle**-P-**X**	2.1 ± 0.1	**13**	Pyr-R-P-R-L-S-H-K-c[**X**-P-**Nle**-P-**X**]c	1.1 ± 0.1
14L	Pyr-R-P-R-L-S-H-K-G-**X**-**Nle**-P-F-**X**	445 ± 62	**14**	Pyr-R-P-R-L-S-H-K-G-c[**X**-**Nle**-P-F-**X**]c	310 ± 59

[a]X represents allylglycine, Rx represents N_α-allyl-arginine, Sx represents N_α-allyl-serine, c[···]c corresponds to the position of the macrocycle along the sequence chain. [b]K_i or dissociation constants were estimated using the Cheng−Prusoff equation and correspond to the concentration of ligand that displaces 50% of radiolabeled [^{125}I] [Nle^{75}, Tyr^{77}] Pyr[1]-apelin-13; value are shown as mean ± SEM of three independent experiments.

plasma ex vivo and a few minutes in vivo, with major cleavage sites mediated by angiotensin-converting enzyme 2 (ACE-2) on the penultimate position (residues Pro[12]-Phe[13]) and neprilysin between residues Arg[4]-Leu[5] or Leu[5]-Ser[6].[35−37] Few approaches have been used to improve the stability of Pyr-apelin-13. Conjugation of fatty acid derivatives or PEG to the N-terminus of apelin increased half-life above 24 h in rat plasma.[38,39] Replacement of residues adjacent to the cleavage sites of ACE 2 (Pro[12], Phe[13]) or neprilysin (Arg[4], Leu[5], or Ser[6]) also contributes to protect against proteolytic degradation.[36,38,40]

Macrocyclization is a recognized method to simultaneously improve the proteolytic stability of peptides and modulate their biological activity and has been successfully applied against several targets including proteases, protein−protein interaction, and GPCRs.[41,42] Few macrocyclization attempts were reported for the apelins, including cyclization between Ser[6] and Pro[12], which improved plasma stability,[43] cyclization between Gln[1] and Ser[6], which provided Gα_i-biased cyclic analogues MM07 (**21**, Figure 1),[44] as well as bicyclic antagonist c[CRPRLC]-KH-c[CRPRLC].[45] More recently, we reported a series of Gα_i-biased macrocycles bearing a Tyr(OBn) residue in position 13 (ring closure between residues His[7] and Met[11]),[46] and Ma et al. provided the first X-ray structure of human APJ receptor in complex with a macrocyclic analogue of apelin-17 (cyclized between residues Ser[6] and Gly[9]).[47]

To date, despite the above, there has been no systematic probing of the impact of apelin-13 cyclization on its biological properties such as binding, stability, and signaling profile. In the present study, cyclization was implemented on every position of Pyr-apelin-13, using an approach reminiscent of the "rolling loop scan" reported by Reichwein et al.,[48] and the impact of such structural modifications on binding affinity, plasma stability, and signaling profiles of the resulting analogues was assessed.

RESULTS AND DISCUSSION

Design of Macrocycles. To build the macrocycles, two amino acids located at the *i*, *i*+4 positions of Pyr-apelin-13 were replaced by allylglycine (Scheme 1), then side chains were connected using ring-closing metathesis (RCM) to generate a series of 17-membered rings. This ring size incorporates three endocyclic amino acids corresponding to the *i*+1, *i*+2, and *i*+3 residues. Similar to previous studies, residue Met[11] was replaced by Nle to avoid sulfur oxidation.[49] Because Arg[2] and Arg[4] are known to be crucial for binding,[7] their side chains were conserved in the N_α-linked macrocycles. In these cases, cyclization was performed with allyl groups introduced on the alpha amine (N_α) via Fukuyama−Mitsunobu allylation,[50,51] generating in fine a tertiary amide (analogues **3**, **6**) (see Supporting Information, Scheme 1S).

Synthesis. Pyr-apelin-13 analogues were synthesized manually using the Fmoc strategy on Wang resin (0.3 mmol·g^{-1}).[52,53] The first amino acid was loaded on resin via a Mitsunobu reaction using triphenylphosphine (PPh_3) and diisopropyl azodicarboxylate (DIAD), then unreacted benzylic alcohols on the resin were capped with acetic anhydride. The Fmoc group was then removed using piperidine in *N*,*N*-dimethylformamide (DMF) (20/80) and the next amino acid, activated by [hexafluorophosphate of *O*-(7-azabenzotriazol-1-yl)-1,1,3,3-tetramethyluronium] (HATU) and diisopropylethylamine (DIPEA) in DMF, was coupled. The full linear sequence was built by repetition of the above steps. Subsequently, RCM was carried out using the Hoveyda−Grubbs second-generation catalyst (HG-II) using the modified protocol of Patgiri et al. (Scheme 1).[54] Briefly, dry resin was swelled with dichloroethane, and dry Ar was bubbled through the mixture for 30 min. The HG-II RCM catalyst was then added, and the reaction mixture heated to 120 °C for 10 min under microwave irradiation. Finally, the peptide was cleaved from the resin using a cocktail of trifluoroacetic acid (TFA)/tri-isopropylsilane (TIPS)/H_2O (95:2.5:2.5). This step was followed by peptide precipitation in *tert*-butyl methyl ether (TBME) and subsequent purification using reverse-phase preparative HPLC coupled to mass spectrometry.

The Fukuyama−Mitsunobu secondary amine synthesis was used to generate *N*-linked macrocycles.[51] Accordingly, the amine group was first nosylated on resin using *o*-nosyl chloride (Supporting Information, Schemes 1S, 2S). The allyl group was then introduced using allylic alcohol, PPh_3, and DIAD. To achieve a higher yield, RCM was preferentially performed immediately after this step rather than at the end of peptide elongation. Peptides were cleaved and purified as above.

DOI: 10.1021/acs.jmedchem.7b01353
J. Med. Chem. 2018, 61, 2266−2277

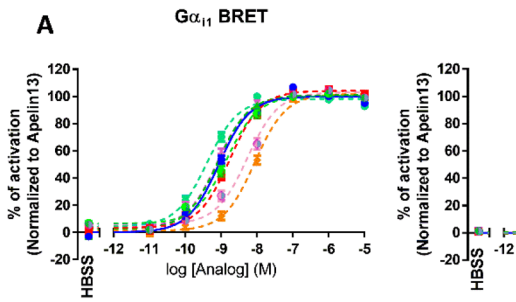

No	K_i (nM)[a]	EC_{50} $G\alpha_{i1}$ (nM)[b]	EC_{50} β-arr2 (nM)[c]
Apc13	0.7 ± 0.1	1.1 ± 0.2	60 ± 4
2L	2.5 ± 0.8	0.4 ± 0.1	35 ± 5
3L	2.9 ± 1.3	5.7 ± 2.4	232 ± 34
5L	1.9 ± 0.2	9.2 ± 2.4	274 ± 82
6L	2.7 ± 0.3	2.1 ± 0.6	91 ± 19
11L	0.3 ± 0.1	1.0 ± 0.4	42 ± 11
12L	2.3 ± 0.2	0.8 ± 0.2	58 ± 11
13L	2.1 ± 0.1	2.0 ± 0.7	145 ± 22

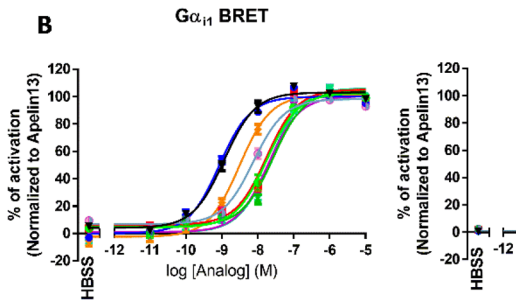

No	K_i (nM)[a]	EC_{50} $G\alpha_{i1}$ (nM)[b]	EC_{50} β-arr2 (nM)[c]
Apc13	0.7 ± 0.1	1.1 ± 0.2	60 ± 4
2	5.7 ± 3.5	23 ± 6	857 ± 195
3	4.5 ± 1.4	6.0 ± 1.4	179 ± 21
5	3.0 ± 0.1	3.7 ± 0.9	126 ± 26
6	9.1 ± 1.4	19 ± 5	512 ± 131
11	1.4 ± 0.4	20 ± 2	400 ± 35
12	14 ± 7	30 ± 7	825 ± 113
13	1.1 ± 0.1	19 ± 4	272 ± 7
15	0.15 ± 0.01	1.3 ± 0.7	57 ± 5

Figure 2. Functional assays of Pyr^1-apelin-13 analogues performed using BRET-based biosensors. Dose−response curves showing the potency in $G\alpha_{i1}$ activation and β-arrestin2 recruitment of linear (A) and macrocyclic (B) analogues. [a](K_i) or ligand/receptor dissociation constants: estimated using the Cheng−Prusoff equation and correspond to the concentration of ligand that displaces 50% of radiolabeled [^{125}I] [Nle^{75}, Tyr^{77}] Pyr^1-apelin-13. [b]EC_{50} $G\alpha_{i1}$: Concentration of ligand producing 50% dissociation of $G\alpha_{i1}$ from $G\beta\gamma$ subunit. [c]EC_{50} β-arr2: concentration of ligand inducing 50% recruitment of β-arrestin2 to the receptor. Values are shown as mean ± SEM of three independent experiments.

Macrocyclization by RCM was generally associated with low-to-medium conversion (15−30%). In particular, precursor **5L** could not be converted to compound **5** even after 2 h microwave irradiation. For this compound, an alternative approach was implemented via cyclization prior to the addition of the Pyr^1-Arg^2 residues. All purified products were characterized by UPLC-MS and high-resolution mass spectrometry (HRMS).

Impact of Macrocyclization on Binding Affinity. In addition to macrocycles, biological activity of the corresponding linear precursors (named with suffix L for linear analogue, Table 1) was assessed to evaluate the respective impact of residue mutation vs cyclization on ligand−receptor binding and signaling (Figure 1).

Several macrocycles possess equivalent or lower affinity for the APJ receptor compared to their linear analogues (Table 1). Interestingly, these differences vary as a function of the macrocyclization position. On the basis of this analysis, the N- and C-termini emerge as the most suitable regions for cyclization [*i*, *i*+4; 17-membered cycle], with compounds **2**, **3**, **5**, **6**, **11**, and **13** displaying K_i values between 1 and 10 nM. It is interesting to note that the APJ receptor is tolerant of modifications to the structure of its ligand in such distant positions, which suggests that these positions are potential sites to further modulate the structure of the ligand.

Macrocyclic analogues modified at the N-terminus displayed only a marginal decrease in affinity compared to their linear counterparts (e.g., **2**, K_i 5.7 nM vs **2L**, K_i 2.5 nM; **3**, K_i 4.5 nM vs **3L**, K_i 2.9 nM; **5**, K_i 3.0 nM vs **5L**, K_i 1.9 nM). The presence of Arg^2 and Arg^4 turned out to be important to preserve affinity, consistent with current knowledge.[7,8,53] As a further testimony of the role of Arg residues, analogue **3** possessing an N_α-allylated Arg^2 residue, with almost the same cyclization position as **4**, displayed a 100-fold higher affinity compared to **4** in which the Arg^2 position is replaced by allylglycine (**3**, K_i 4.5 nM vs **4**, K_i 509 nM). Likewise, macrocycle **6** bearing an N_α-allylated Arg^4 residue is 600-fold more potent than **7** in which Arg^4 is replaced by allylglycine (**6**, K_i 9.1 nM vs **7**, K_i 6074 nM). Compared with the well-studied macrocyclic compound **21**, cyclized between Gln^1 and Ser^6 residues (K_i 48 nM),[44] compounds **2** and **3** in this series bearing similar cyclization showed 5−10-fold improved binding affinities. One possible explanation is that **21** possesses a larger ring incorporating more residues (additional Ser^6 residue compared to **2**, and additional Pyr^1 residue compared to **3**), which may impact orientation of the RPRL pharmacophore.

On the other hand, macrocyclization in the central portion of Pyr-apelin-13 was detrimental on binding affinity. Analogues **7** and **8** possessed 1 order of magnitude lower binding affinity compared to their respective linear analogues (**7**, K_i 6074 nM vs **7L**, K_i 489 nM; **8**, K_i 41 nM vs **8L**, K_i 3.9 nM) (Table 1). This is consistent with previous studies whereby *N*-methylation of amide bonds induced a significant loss of potency in activity reporter assay using stably expressing recombinant human APJ-$G\alpha_{16}$ cell line.[39] Taken together, these results suggest that the central part of Pyr-apelin-13 must adopt a well-defined conformation distinct from that imposed by the current cyclization approach. A promising macrocyclic template for this position is AMG-3054 (**22**) (reported by Ma et al.), which features a larger ring and was nonetheless cyclized between Ser^6 and Gly^9, albeit on an apelin-17 scaffold.[8,47]

Among this set of compounds, C-terminally modified macrocycles **11**−**13** exhibited high affinity for the APJ receptor, with analogue **13** possessing the highest affinity (K_i 1.1 nM), similar to its linear congener (**13L**, K_i 2.1 nM). Knowing that the C-terminal interacts deeper in the transmembrane domain,[47] this data suggests a large binding pocket able to accommodate the 17-membered ring. The substitution of the Pro^{10} residue by an allylglycine was also detrimental for ligand binding affinity, irrespective of cyclization site (**9**, K_i 188 nM vs **9L**, K_i 41 nM; **10**, K_i 268 nM vs **10L**, K_i 194 nM; **14**, K_i 310 nM vs **14L**, K_i 445 nM).

DOI: 10.1021/acs.jmedchem.7b01353
J. Med. Chem. 2018, 61, 2266−2277

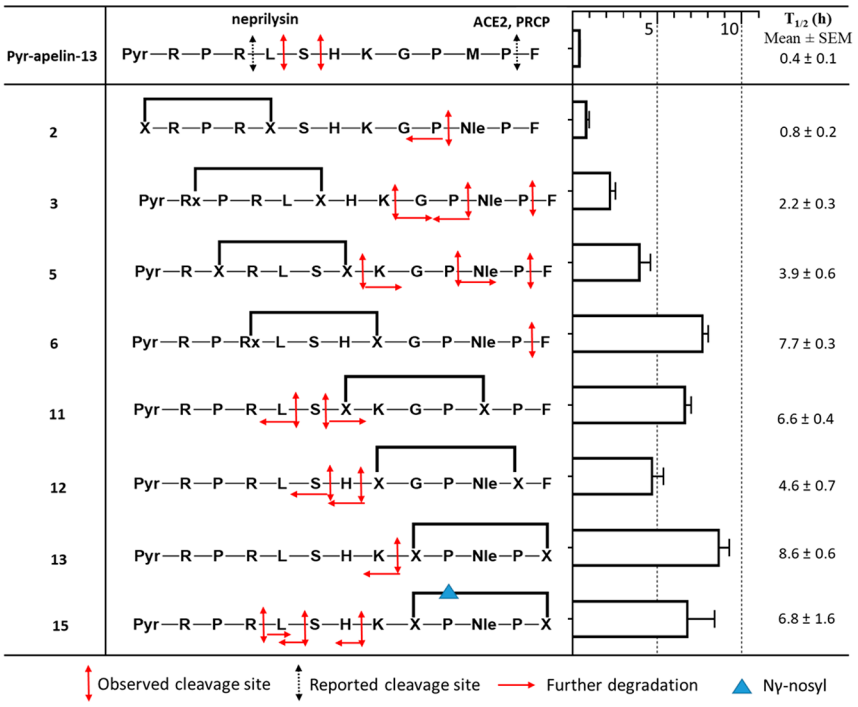

Figure 3. Half-lives and cleavage sites of apelin-13 analogues. X represents allylglycine, Nle represent norleucine, and Rx represents *N*-allyl-arginine. Half-life values were determined as means ± SEM of three independent experiments.

Impact of Macrocyclization on Signaling. The signaling profile of the most promising analogues (K_i < 30 nM) was assessed using bioluminescence resonance energy transfer (BRET) assays in HEK cells expressing the human APJ receptor, with a particular emphasis on activation of $G\alpha_{i1}$ (canonical pathway of the APJ receptor leading to intracellular cAMP reduction)[17] and recruitment of β-arrestin2 (associated with receptor internalization).[55] Macrocycles and their linear analogues were divided into two groups based on their ability to modulate APJ receptor signaling (Figure 2).

The first group consists of most analogues for which cyclization showed a deleterious effect on receptor signaling (**2**, **6**, **11**, **12**, **13**). When linear compounds displayed similar potencies as Pyr-apelin-13, cyclization induced a 10−40-fold loss in $G\alpha_{i1}$ activation (**2**, EC_{50} $G\alpha_{i1}$ 23 nM vs **2L**, 0.4 nM) and 5−25-fold decrease in β-arrestin2 recruitment (**2**, EC_{50} β-arr2 834 nM vs **2L**, 35 nM).

The second group includes analogues where cyclization showed beneficial effects on signaling properties (compounds **3**, **5**). While the linear compound **5L** induced a significant decrease in downstream signaling activation compared to Pyr-apelin-13, macrocyclization slightly restored potency on both pathways (**5**, EC_{50} $G\alpha_{i1}$ 3.7 nM vs **5L**, 9.2 nM; the same for β-arrestin2).

Structurally, the Arg^2 -Pro^3-Arg^4-Leu^5 moiety has been altered in analogues **3L** and **5L**. N_α-Allylation was introduced on residue Arg^2 in **3L**, and residue Pro^3 was replaced by allylglycine in **5L**. Because the N-terminus of apelin was shown by NMR and molecular modeling to be ordered, with a putative β-turn structure,[56,57] modifications such as amino acid substitution would be expected to disrupt this secondary structure and impact intracellular signaling. As a matter of fact, hydrogen bonding with the backbone is often critical in maintaining peptide secondary structure.[58] Despite this, compound **3L**, which cannot form a critical H-bond by virtue of N_α-allylation, showed a modest decrease in binding affinity and signal transduction. This is in agreement with previous studies showing that amide bond methylation between Pyr^1-Arg^2 and Pro^3-Arg^4 did not affect Ca^{2+} mobilization.[39] Accordingly, this structural moiety seems to be more governed by Pro^3 rather than intramolecular H-bonds. Indeed, replacement of Pro^3 by allylglycine led to decrease in $G\alpha_{i1}$ activation and β-arrestin2 recruitment (compound **5L**). Interestingly, macrocyclization on this position either had a neutral impact (compound **3** vs **3L**), or marginally improved potency compared to its linear analogue (compound **5** vs **5L**).

Impact of Macrocyclization on Plasma Stability. The influence of macrocyclization on plasma stability was then assessed via incubation of compounds in rat plasma followed by UPLC-MS analysis at selected time points (0, 2, 4, 7, and 24 h or 0, 10, 20, 60, and 120 min). Half-lives and observed cleavage sites of the most active analogues are reported in Figure 3 (for other compounds, see Supporting Information, Figure 1S). Previous work on linear analogues of Pyr-apelin-13 showed that substitutions next to the critical proteolytic site increased peptide stability, however, half-lives of those linear analogues were usually less than 2 h.[36] In this study, macrocycles displayed significant improvements in plasma stability, and the protection offered by cyclization critically depends on their position.

Cyclization in the central and C-terminus portions of the peptide were the most beneficial, with $t_{1/2}$ > 3 h compared to 0.4 h for Pyr-apelin-13. Particularly, compounds **6** and **13** possessed $t_{1/2}$ 7.7 and 8.6 h, respectively. Compound **13** ($t_{1/2}$ 8.6 h) was also more stable than its linear counterpart **13L** ($t_{1/2}$ 2.4 h). At the same cyclization position, N_α-linked macrocyclic analogues displayed even longer half-lives (**3**, $t_{1/2}$ 2.2 h vs **4**, $t_{1/2}$ 0.7 h), (**9**, $t_{1/2}$ > 24 h vs **10**, $t_{1/2}$ 4.1 h) (Supporting Information, Figure 1S).

DOI: 10.1021/acs.jmedchem.7b01353
J. Med. Chem. 2018, 61, 2266−2277

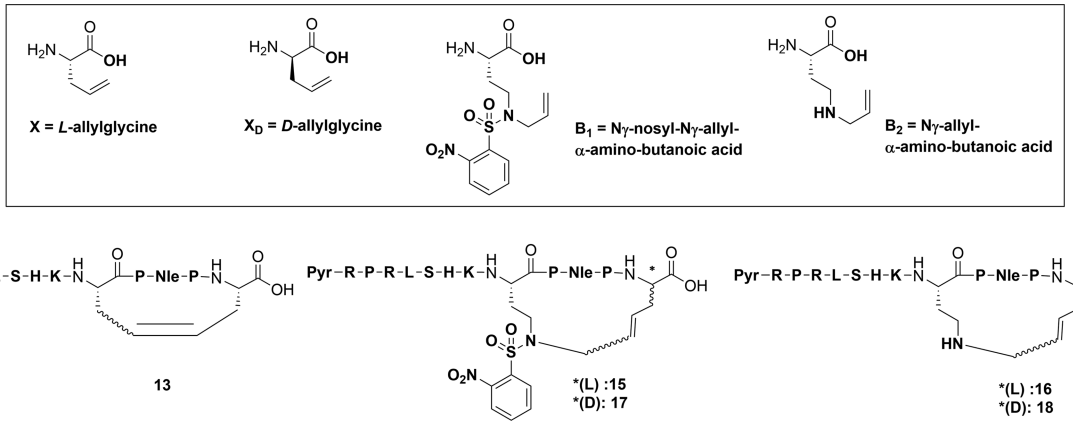

Figure 4. C-Terminally modified macrocyclic analogues of compound **13**.

Table 2. Affinity and Signaling Profiles of C-Terminally-Modified Macrocyclic Analogues of Compounds 13

	peptide sequence[a]	binding K_i (nM)[b]	$G\alpha_i$ EC_{50} (nM)[c]	β-arr2 EC_{50} (nM)[d]
Ape13	Pyr-R-P-R-L-S-H-K-G-P-M−P-F	0.7 ± 0.1	1.1 ± 0.2	60 ± 4
5	Pyr-R-c[**X**-R-L-S-**X**]c-K-G-P-**Nle**-P-F	3.0 ± 0.1	3.7 ± 0.9	126 ± 26
13	Pyr-R-P-R-L-S-H-K-[**X**-P-**Nle**-P-**X**]	1.1 ± 0.1	19 ± 4	272 ± 7
15	Pyr-R-P-R-L-S-H-K-[**B_1**-P-**Nle**-P-**X**]	0.15 ± 0.01	1.3 ± 0.7	57 ± 5
16	Pyr-R-P-R-L-S-H-K-[**B_2**-P-**Nle**-P-**X**]	917 ± 93		
17	Pyr-R-P-R-L-S-H-K-[**B_1**-P-**Nle**-P-**Xd**]	0.10 ± 0.01	1.7 ± 0.8	63 ± 10
18	Pyr-R-P-R-L-S-H-K-[**B_2**-P-**Nle**-P-**Xd**]	206 ± 29		
19	NH_2-[B_1-P-Nle-P-X]	>10000		
20	NH_2-[B_2-P-Nle-P-Xd]	>10000		

[a]X represents allylglycine, Xd represents D-allylglycine, Nle represents norleucine, B_1 represents *Nγ*-nosyl-*Nγ*-allyl-*α*-amino-butanoic acid, B_2 represents *Nγ*-allyl-*α*-amino-butanoic acid, c[···]c represents the position of the macrocycle in the chain. [b](K_i) or dissociation constants were estimated using the Cheng−Prusoff equation and correspond to the concentration of ligand that displaces 50% of radiolabeled [^{125}I] [Nle^{75}, Tyr^{77}] Pyr^1-apelin-13. [c]EC_{50} $G\alpha_{i1}$ corresponds to the concentration of ligand producing 50% dissociation of $G\alpha_{i1}$ from $G\beta\gamma$ subunit. [d]EC_{50} β-arr2 is the concentration of ligand inducing 50% recruitment of β-arrestin2 to the receptor. Values was showed as mean of three independent experiments.

Regarding cleavage sites, no endocyclic cleavage was observed. Moreover, most analogues were cleaved between Arg^4 and Phe^{13}, confirming that macrocyclization in this region protects the peptide from proteolysis, which substantially improves its stability (Supporting Information, Figure 1S). The previously reported cleavage sites identified on apelin-13 were also observed in this study, except when endocyclic. ACE2-mediated cleavage between Pro^{12} and Phe^{13} was observed on **3**−**7**, **9**, **10**; cleavage between Ser^6 and His^7 was observed on **11** and **12**,[36] and cleavage between either Arg^4-Leu^5 (on **8**−**10**) or Leu^5-Ser^6 (on **9**−**11**, **14**), recently reported to be mediated by neprilysin,[36,37] was also observed.

In the C-terminus, fragments corresponding to cleavage between His^7-Lys^8 (on **4**, **5**, **12**) and Pro^{10}-Nle^{11} (on **2**−**5**) were also observed, consistent with previously reported cleavage sites of apelin-13 analogues.[36] Some new cleavage sites were observed in the current study, such as between Lys^8-Gly^9 on macrocycles **3**, **7**, **13**.

In the above analysis, one should keep in mind that the absence of an observable fragment does not necessarily mean that this fragment was not produced; instead, it may undergo subsequent cleavage to a smaller fragment. The aforementioned cleavage sites may also exist on Pyr-apelin-13, however, were not reported to date. For example, in our previous studies, replacement of selected residues of Pyr-apelin-13 with unnatural amino acids to prevent the cleavage between Leu^5-Ser^6, revealed the presence of another cleavage site between His^7-Lys^8.[36] This cleavage site was again found in this series of macrocycles (**4**, **5**, **12**).

Exploring the Binding Pocket with Larger Macrocycles. To further investigate the properties of the binding pocket, several analogues of **13** [macrocycle linked X^9-X^{13}; 17-membered ring] were built, in which size and linker type were modified (Figure 4). Results reveal that enlarging macrocycle size up to 20 atoms with no additional endocyclic amino acid [B^9-X^{13}; 20-membered ring] improved binding affinity compared to Pyr-apelin-13 (K_i 0.7 nM). This modification led to the most potent macrocyclic analogues in this study, analogues **15** (K_i 0.15 nM) and **17** (K_i 0.10 nM) (Table 2). These also exhibit similar properties in terms of $G\alpha_{i1}$ signaling (**15**, EC_{50} 1.3 nM; **17**, EC_{50} 1.7 nM) and β-arrestin2 recruitment (**15**, EC_{50} 57 nM; **17**, EC_{50} 63 nM) as apelin-13 (EC_{50} $G\alpha_{i1}$ 1.1 nM and EC_{50} β-arr2 60 nM). Furthermore, compound **15** displays significant improvements in plasma stability compared to apelin-13 with $t_{1/2}$ 6.8 h (Figure 3).

The only difference between **15** and **17** is the chiral center on amino acid 13. **15** features an L-allylglycine^{13} linker in position 13, whereas **17** carries a D-allylglycine^{13}. This modification does not induce a major difference in affinity between the two compounds, contrasting with the 20-fold decrease observed when substituting L-Phe^{13} by D-Phe^{13} on Pyr-apelin-13 from a previous study.[49] One difference between these two sets of results is the presence of the 2-nitrobenzenesulfonamide (*o*-nosyl) on the side chain of position 9, which may provide an additional energetically

DOI: 10.1021/acs.jmedchem.7b01353
J. Med. Chem. 2018, 61, 2266−2277

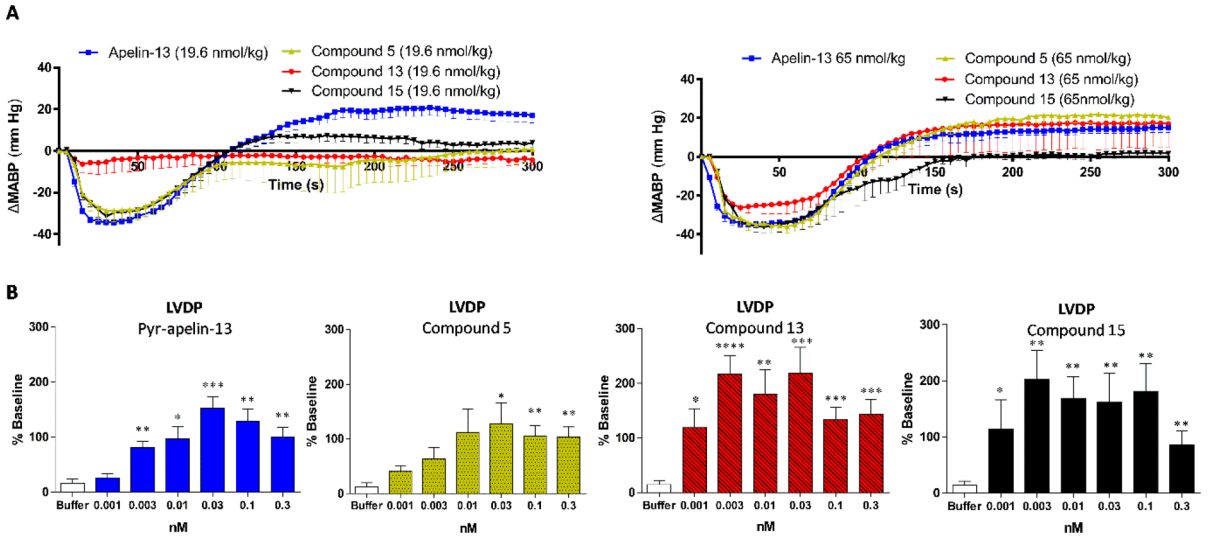

Figure 5. Hypotensive effect in vivo on anesthetized rats and left ventricular developed pressure (LVDP) effect ex vivo on rat isolated-perfused heart of Pyr[1]-apelin-13, compounds **5**, **13**, and **15**. (A) Tracings depict the variation of blood pressure upon iv administration of a bolus injection of compounds at two doses 19.6 and 65 nmol/kg via the jugular vein. (B) Tracings describe the LVDP induced by compounds with increasing doses from 0.001 to 0.3 nM. * $p < 0.05$, ** $p < 0.01$, *** $p < 0.001$, **** $p < 0.0001$ vs buffer. Data was analyzed using unpaired and parametric *t* test.

favorable interaction with the receptor. On the basis of the X-ray structure of the APJ receptor,[47] the space between side chains of residues 9 and 13 is an aromatic cage composed of residues from the N-terminus (Trp^{24}), transmembrane domains I (Tyr^{35}), II (Trp^{85}, Tyr^{93}, Tyr^{88}) and VII (Phe^{291}), which creates potential opportunities for $\pi-\pi$ interaction with electron-deficient moieties such as the *o*-nosyl group. Accordingly, removal of the nosyl group on the same macrocycles results in a 6000-fold decrease (**16**, K_i 917 nM) and 2000-fold decrease (**18**, K_i 206 nM) in binding affinity compared to nosylated analogues (**15** and **17**), respectively. The newly created positive charge of the amine on the linker in **16** and **18** may be contributive to such loss in this essentially hydrophobic pocket.[47,49] Finally, truncation of the N-terminal portion of **15** and **17** completely abolished their affinity for the APJ receptor (**19** and **20**, K_i > 10000 nM), which emphasizes the importance of this portion for ligand binding. Thus, ring enlargement by itself was beneficial only in the presence of the *N*-nosyl group.

Regarding degradation profile, there are differences in cleavage sites between **13** and **15** despite identical macrocyclization position (Figure 3). The cleavage site of neprilysin (Arg^4-Leu^5, Leu^5-Ser^6) and those between His^7-Lys^8 were identified on **15**, whereas the only cleavage site identified on **13** was between Lys^8 and the macrocycle core. This suggests that ring size or linker type may influence the interaction between peptides and proteases. However, the half-life of the two peptides is not significantly different and it should be kept in mind that several fragments may not be identified due to subsequent cleavages.

Effect of Macrocyclic Analogues on Blood Pressure and Cardiac Performance in Rats. The N- and C-terminally modified macrocycles **5**, **13** and **15**, with the highest binding affinity and potency on the $G\alpha_{i1}$ and β-arrestin2 pathways in this collection, were tested for their ability to modulate blood pressure in vivo and to modify cardiac contractility in the Langendorff isolated heart perfusion assay ex vivo (Figure 5).

Blood pressure was monitored after iv bolus administration of two doses (19.5 and 65 nmol/kg) of compounds **5**, **13**, and **15** to anesthetized rats. Our results revealed that compounds **5** and **15** present similar hypotensive effects to Pyr-apelin-13, inducing rapid and robust blood pressure lowering up to 40 mmHg. As opposed to **5** and **15**, compound **13** appears less potent, inducing blood pressure drop only at the highest dose tested. Given that previous studies suggested a link between hypotension and receptor internalization,[8] we next assessed APJ internalization after stimulation with either apelin-13, **13**, or **15** using enzyme-linked immunosorbent assay (ELISA) (Figure 6).

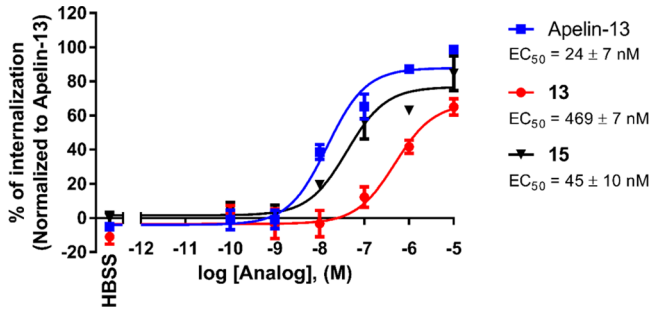

Figure 6. Internalization assay of compounds **13** and **15** using ELISA. EC_{50}: concentration of ligand inducing internalization of 50% HA-tagged receptor. Values are shown as mean ± SEM of three independent experiments.

Results indicate that **13** (EC_{50} 469 nM) is 10-fold less potent than its analogues **15** or Pyr-apelin-13 (EC_{50} 45 and 24 nM, respectively) to induce receptor internalization, consistent with its lower ability to modulate blood pressure. It was also noted that the hypertensive phase observed with Pyr-apelin-13 (presumably due to baroreflex activation), was not observed following iv administration of compound **15**, even at the highest dose. Interestingly, although replacement of Phe^{13} by alanine in previous studies yielded a physiological antagonist devoid of hypotensive effect,[59] analogues **13** and **15**, devoid of an aromatic residue in position 13, still display an agonist profile in vivo.

DOI: 10.1021/acs.jmedchem.7b01353
J. Med. Chem. 2018, 61, 2266−2277

Despite longer half-life in vitro, the hypotensive action of **13** and **15** lasted no longer than 5 min in this test, similarly to other APJ receptor agonists.[20] This may tentatively be explained with several factors. First, internalization and desensitization of the APJ receptor could contribute to reduce the duration of action of agonists.[55] Moreover, although they display higher stability in plasma ex vivo, their elimination and metabolism in vivo may reduce circulating concentrations and hence their effect. To assess this latter point, we performed a preliminary pharmacokinetic analysis in which apelin-13, **13**, and **15** were administered to rats iv at 3 mg/kg (Supporting Information, Figure 2S). Results of this study show that both **13** and **15** display significantly higher circulating concentrations and AUC (**13**, AUC 246 μg/mL·min; **15**, 168 μg/mL·min) compared to Pyr-apelin-13 (AUC 0.2 μg/mL·min). While the hypotensive phase ends 2−3 min after administration for the three compounds, the remaining quantity at 5 min (**13**, 8.4 μg/mL or 5.6 μM; **15**, 4.3 μg/mL or 2.5 μM) are sufficient to saturate the available APJ receptors (**13**, K_i 1.1 nM; **15**, K_i 0.15 nM). This finding suggests that the rapid normalization of blood pressure may not relate to circulating concentrations, but other factors, such as receptor desensitization or the baroreflex, which liberates vasoconstrictor agents such as catecholamines.[60]

To evaluate the ability of new analogues to modulate cardiac function in the Langendorff model, the heart of Sprague−Dawley rats was isolated and perfused with different concentrations of macrocyclic analogues, with doses ranging from 0.001 to 0.3 nM. In this experiment, the increase in left ventricular developed pressure is recorded as a measure of inotropic effect.[61] Results showed that compounds **13** and **15** behave as powerful cardiostimulants. Indeed, both compounds demonstrated increased potency (with maximum response at a concentration of 0.003 nM as opposed to 0.03 nM for Pyr-apelin-13), as well as increased efficacy (compound **13** reaching 217 ± 33% from baseline compared to 81 ± 11% from baseline for Pyr-apelin-13 at dose of 0.003 nM, $p < 0.001$). On the other hand, macrocycle **5** possessed similar potency and efficacy to Pyr-apelin-13.

CONCLUSION

This study reports the first systematic study of the influence of macrocyclization on binding affinity, signaling profiles, plasma stability, and ex vivo and in vivo cardiovascular effects of macrocyclic analogues of Pyr-apelin-13. By moving the site of ring closure along the sequence, several positions appeared suitable for macrocyclization on the N- and C-termini of apelin-13. The 17-membered C-terminal macrocycle **13** possesses a comparable binding affinity for the APJ receptor compared to its linear analogue. Enlarging the ring led to **15** and **17** possessing higher affinity (**15**, K_i 0.15 nM; **17**, K_i 0.10 nM or 5−7-fold higher than Pyr-apelin-13). The signaling profile of high-affinity analogues was established using BRET-based assays. In terms of $G\alpha_{i1}$ activation and β-arrestin2 recruitment, macrocyclization was detrimental on most positions, except for the nosylated analogues **15** and **17**. Furthermore, in the Arg^2-Pro^3-Arg^4-Leu^5 moiety, whereas linear analogues lost their potency due to Pro^3 replacement (**5L**), macrocyclization was beneficial by partially restoring potency for both pathways (**5**). Regarding plasma stability, the sequence between Arg^4-Phe^{13} seems optimal for cyclization, protecting the peptide from degradation. Accordingly, **13** possesses a longer half-life in rat plasma (8.6 h) compared to Pyr-apelin-13 (24 min) and its linear analogue **13L** (2.4 h). This translated into higher circulating concentrations in rats in vivo. Finally, the impact of compounds on blood pressure and on the isolated-perfused heart ex vivo suggest that compounds **13** and **15** are powerful modulators of the cardiovascular system. Altogether, these new macrocycles represent useful pharmacological tools to better rationalize the links between signaling profile and physiological action and more broadly the pharmacophysiology of the apelinergic system.

EXPERIMENTAL SECTION

Chemistry. *Materials.* Wang resin (maximum loading 0.5−1.0 mmol/g, particle size 200−400 mesh), diisopropylethylamine (DIPEA), trifluoroacetic acid (TFA), and amino acids were purchased from Chem-Impex International (Wood Dale, USA). Polypropylene cartridges 12 mL with 20 μm PE fit were purchased from Applied Separation (Allentown, USA), and HATU was ordered from Matrix Innovation (Québec, Canada). Other reagents and solvent were purchased from Sigma-Aldrich (Missouri, USA) and Fisher Scientific (Hampton, USA). The above reagents and solvents were used as received.

*Solid Phase Synthesis (Compounds **1−20** and **2L−14L**).* All peptides were synthesized at 0.1 mmol scale on Wang resin (loading 0.3 mmol/g). For the loading step, resin was first swelled in 4 mL of anhydrous tetrahydrofuran (THF) for 5 min. Fmoc-protected amino acid (0.3 mmol) and triphenylphosphine (78 mg, 0.3 mmol) were then added, and the mixture was shaken for another 5 min. A solution of DIAD (60 μL, 0.3 mmol) in 1 mL of anhydrous THF was added slowly, and the reaction mixture agitated overnight on an orbital shaker at 120 rpm. The resin was then filtered and washed with a sequence of DMF-DCM-iPrOH-DCM-iPrOH-DCM (5 mL solvent, 3 min cycles). Unreacted benzylic groups were capped using 5 mL of a solution of acetic anhydride−DIPEA−DCM (4:1:0.2). For amino acid coupling, the Fmoc group was first removed by treating with 20% piperidine/DMF (5 mL, 2 × 10 min), and the resin was washed again with the above washing sequence. The Fmoc-protected amino acid (0.5 mmol) was then added as a solution with HATU (190 mg, 0.5 mmol) and DIPEA (87 μL, 0.5 mmol) in 5 mL of DMF, and the mixture was shaken for 30 min. Upon completion of the reaction, the resin was washed again with the above washing sequence. Deprotection and coupling steps were repeated to produce the full linear sequence. Finally, the resin was washed with diethyl ether and dried in a vacuum desiccator prior to the metathesis step.

*Ring Closing Metathesis (Compounds **2−20**).* Dry resin (0.1 mmol peptide) was placed in a 10 mL microwave tube equipped with a stirring bar, then 3 mL of anhydrous 1,2-dichloroethane was added to swell the resin. This suspension was purged with argon for 30 min. Subsequently, 15 mg (0.023 mmol) of Hoveyda−Grubbs second-generation catalyst was added. The reaction mixture was agitated, purged with argon for 5 min, and submitted to microwave irradiation in a Discover SP microwave oven (CEM, Matthews, USA) with the following parameters: controlled temperature 120 °C, time 10 min, maximum power 300 W. The resin was filtered and washed with the washing sequence DCM-MeOH-DCM-MeOH-DCM (5 mL, 3 min each). Final cleavage from the resin and simultaneous side chain deprotections were performed with 4 mL of a TFA−TIPS−H_2O (95:2.5:2.5) mixture for 4 h, then the crude product was precipitated in 35 mL of TBME at 0 °C, centrifuged at 2000 rpm for 10 min, and isolated as a light-brown solid after removal of the supernatant.

For compounds **3**, **5**, **6**, **9**, and **15−20**, the procedure was slightly modified as described in Supporting Information (Schemes 1S, 2S).

Peptide Purification. The crude product was resuspended in acetic acid 10% and purified on a preparative HPLC-MS system from Waters (Milford, USA) (column XSELECT CSH Prep C18 (19 mm × 100 mm) packed with 5 μm particles, UV detector 2998, MS SQ detector 2, sample manager 2767, and a binary gradient module) using acetonitrile and water + 0.1% formic acid as eluents. Pure fractions were lyophilized to give the final product as a white solid. For purity assessment, compounds were analyzed on a UPLC-MS system from Waters (Milford, USA) (column Acquity UPLC CSH C18 (2.1 mm ×

DOI: 10.1021/acs.jmedchem.7b01353
J. Med. Chem. 2018, 61, 2266−2277

50 mm) packed with 1.7 μm particles) with the following gradient: acetonitrile and water with 0.1% HCOOH (0 → 0.2 min, 5% acetonitrile; 0.2 → 1.5 min, 5% → 95%; 1.5 → 1.8 min, 95%; 1.8 → 2.0 min, 95% → 5%; 2.0 → 2.5 min, 5%). All compounds have ≥95% purity, except **7L** (≥90% purity) and **9L** (≥87%). HRMS of all analogues were obtained using electrospray infusion on a maXis ESI-Q-Tof apparatus from Bruker (Billerica, USA).

In Vitro and in Cellulo Assays. *Materials.* High glucose Dulbecco's Modified Eagle Medium (DMEM), G418, and penicillin/streptomycin, were ordered from Invitrogen Life Technologies (Carlsbad, USA). Fetal bovine serum (FBS) was obtained from Wisent (Saint-Jean-Baptiste, Canada) and bovine serum albumin (BSA) from BioShop (Burlington, Canada). Polyethylenimine (PEI) was obtained from Polysciences (Warminster, USA).

Cell Culture. Human embryonic Kidney cells (HEK293) stably transfected of YFP-tagged human APJ receptor was cultured in DMEM medium with 10% of FBS. Cells were incubated at 37 °C in a humid atmosphere maintaining 5% CO_2. G418 (400 μg/mL) was used to maintain selection pressure for receptor expressed cells, and penicillin/streptomycin (0.1%) were added to prevent bacteria contamination.

Binding Experiment. The binding experiments were carried out on cell membranes. For membrane preparation, HEK293 cells stably expressing the YFP-tagged human APJ receptor were submitted to a freeze−thaw cycle to break down the cells. Lysed cells were gently transferred to a falcon tube containing 4 mL of resuspension solution (1 mM EDTA and 50 mM Tris-HCl, pH 7.4), and cell membranes were pulled down by centrifugation at 3500 rpm for 15 min at 4 °C. The precipitate was resuspended in binding buffer (50 mM Tris-HCl, 0.2% BSA, pH 7.4). Competition binding assay was performed in 96-well plates where 15 μg of membrane proteins were incubated with 0.2 nM of radiolabeled [^{125}I] [Nle^{75}, Tyr^{77}] Pyr-apelin-13 (820 Ci/mmol) and test ligand with concentrations ranging from 10^{-5} to 10^{-11} nM (or 10^{-4} to 10^{-10} nM for compounds with low affinity) in a total volume of 200 μL for 1 h at room temperature. Unbound ligands were removed by filtration through glass fiber filter (Millipore, preabsorbed of PEI 0.5% for 2 h at 4 °C) and then washed three times with 120 μL of binding buffer. The gamma emission was then recorded using γ-counter 1470 Wizard from PerkinElmer (Waltham, USA) (80% efficiency). Nonspecific binding, determined in the presence of 10^{-5} nM of unlabeled Pyr-apelin-13, was not in excess over 5% of total signal. Results were plotted on a concentration−response curve using GraphPad Prism 7 to calculate the IC_{50} values, which represent the concentration of testing ligand displaced 50% of radiolabeled ligand from the receptor. Dissociation constant K_i was calculated from the IC_{50} value using the Cheng−Prusoff equation, and results were showed as mean ± SEM of three independent experiments.[62]

BRET Assays. HEK293 cells seeded in T175 flasks were allowed to grow in high glucose DMEM supplemented with 10% FBS, 100 U/mL penicillin/streptomycin, 2 mM glutamine, and 20 mM HEPES at 37 °C in a humidified chamber at 5% CO_2. All transfections were carried out with polyethylenimine. After 24 h, cells were transfected with the plasmids coding for hAPJ, $G\alpha_{i1}$-RlucII(91), GFP10-$G\gamma_2$, and $G\beta_1$ (from cDNA.org) (for BRET based $G\alpha_{i1}$ activation assay) or coding for hAPJ-GFP10 and RlucII-β-arrestin 2 using polyethylenimine.[53,63,64] To perform BRET assays, cells were transferred into white 96-well plates BD Bioscience (Mississauga, Canada) at a concentration of 50000 cells/well 24 h after transfection and incubated at 37 °C overnight. Cells were then washed with PBS, and 90 μL of HBSS was added in each well. Then, cells were stimulated with analogues at concentrations ranging from 10^{-5} M to 10^{-11} M for 5 min at 37 °C ($G\alpha_{i1}$) or for 30 min at RT (β-arrestin 2). After stimulation, 5 μM of coelanterazine 400A was added to each well and the plate was read using the BRET^2 filter set of a GeniosPro plate reader (Tecan, Austria). The BRET^2 ratio was determined as $GFP10_{em}/RlucII_{em}$. Data were plotted and EC_{50} values were determined using GraphPad Prism 7. Each data point represents the mean ± SEM of at least three different experiments each done in triplicate.

Rat Plasma Stability Assay. Plasma was obtained from male rats by centrifugation of blood at 13000 rpm during 5 min at 4 °C. Synthetic analogues (6 μL of 1 mM aqueous solution) were incubated with plasma (27 μL) at 37 °C for 2, 4, 7, 24 h (or 10, 20, 60, and 120 min for compounds having shorter half-life). Enzymatic reactions were stopped by adding 70 μL of acetonitrile−ethanol (1:1) solution containing nicotinamide 0.5 μM (internal standard).[39] This mixture was then vortexed and centrifuged at 13000 rpm for 20 min at 4 °C. The supernatant was filtered through a 4 mm nylon 0.2 μm filter, diluted with 40 μL of distilled water, and analyzed using Acquity UPLC-MS system class H (CSH C18 column packed with 1.7 μm particles). Percentage of peptide remaining was plotted on an exponential decay curve using GraphPad Prism 7 for calculating half-life. MS spectra at different time points were compared with those at 0 min (rat plasma inactivated by quenching solution before adding compound) to identify cleavage fragments.

Assessment of Internalization by Enzyme-Linked Immunosorbent Assay (ELISA). HEK293 cells were seeded in 24-well plates precoated with 0.1 mg/mL poly-L-lysine (sigma) at 200000 cells/well. Then 48 h post-transfection with the human HA-tagged APJ receptor, cells were washed and stimulated with compounds at concentrations ranging from 10^{-5} to 10^{-11} M for 30 min at 37 °C in HBSS. Cells were then fixed in 3.7% (v/v) formaldehyde/Tris-buffered saline (TBS) (20 mM Tris-HCl, pH 7.5, and 150 mM NaCl) for 5 min at room temperature. Cells were then washed twice with TBS and incubated 30 min with TBS containing 1% BSA at room temperature to block nonspecific binding. A monoclonal anti-HA-peroxidase antibody (clone 3F10, Roche Applied Sciences) was then added at a dilution of 1:1000 in TBS-BSA 1% for 60 min. Following the incubation with the primary antibody, cells were washed twice with TBS and 250 μL of 3,3′,5,5′-tetramethylbenzidine (Sigma-Aldrich, Canada) were added. The plates were incubated at room temperature, and the reaction was stopped using 250 μL of HCl 2N. Then 200 μL of the colorimetric reaction was transferred to a 96-well plate and the absorbance was measured at 450 nm. Cells transfected with empty vector were used to determine background. Data were plotted and EC_{50} values were determined by using GraphPad Prism 7. Each data point represents the mean ± SEM of at least three different experiments. The optical density (DO) measured at 1 μM for **13** or **15** was normalized to the DO measured at 1 μM for Pyr-apelin-13, providing the percentage of internalization induced by these compounds versus Pyr-apelin-13, set at 100% as the reference.

In Vivo and Ex Vivo Assays. Adult male Sprague−Dawley rats were purchased from Charles River Laboratories (St-Constant, Quebec, Canada) and maintained on a 12 h light/12 h dark cycle with access to food and water ad libitum. The experimental procedures in this study conformed with the Animal Care Committee of Université de Sherbrooke and in accordance with policies and directives of the Canadian Council on Animal Care.

Blood Pressure Test. Male Sprague−Dawley rats (250−350g) were anesthetized with an intramuscular injection of ketamine/xylazine solution (87/13 mg/kg) and placed in supine position on a thermostatic pad. To measure systemic arterial blood pressure, a catheter (PE 50 filled with heparinized saline) was inserted into the right carotid artery and connected to a Micro-Med transducer (model TDX-300, Calabasas, USA) linked to a Micro-Med blood pressure analyzer (model BPA-100c). Another catheter (PE10) was inserted into the left jugular vein for bolus injection of vehicle (isotonic saline), followed 5 min later by the injection of either Pyr-apelin-13 or macrocyclic analogues (given at 19.6 or 65 nmol/kg; volume of 0.25 mL over 10 s). The iv catheter was flushed with saline (0.3 mL) immediately after each injection to remove residual injected substances. Only one analogue was given per experiment.

Ex Vivo Heart Contractile Function. Hearts from male Sprague−Dawley rats were excised and cannulated through the aorta connected to a Langendorff apparatus. Contractile function was recorded through a saline-filled latex balloon inserted into the left ventricle. Left ventricular pressure was continuously monitored through a precalibrated physiological pressure transducer (Molecular Devices, Sunnyvale, USA). Thereafter, incremental concentrations of either APLN-13 or macrocyclic compounds 0.001−0.3 nM, were infused. Data for left ventricular developed pressure (LVDP) were collected

DOI: 10.1021/acs.jmedchem.7b01353
J. Med. Chem. 2018, 61, 2266−2277

and processed using the Clampfit 10.2 program (Molecular Devices, Sunnyvale, USA)

In Vivo Pharmacokinetic Analysis. Male Sprague−Dawley rats (250−350g) were anesthetized with the same protocol described in the blood pressor test. Compounds (dissolved in 350 μL in normal saline) were administered via the jugular vein at a dose of 3 mg/kg, and blood samples were collected from the carotid artery into EDTA-coated tubes (Sarstedt, Nümbrecht, Germany) at 1, 5, 10, 15, 30, 60, and 120 min (1, 2, 5, 10, and 15 min for pyr-apelin-13) after administration. To remove blood cells, samples were immediately centrifuged at 13000 rpm for 5 min at 4 °C, and the supernatant (plasma) was transferred to a microtube. To the plasma (100 μL) was added acetonitrile (200 μL) containing 1.5 μM internal standard. **13** was used as internal standard for analyses of Pyr-apelin-13, and **15** was used as internal standard for analyses of **13**. This mixture was vortexed, centrifuged at 13000 rpm for 20 min, and filtered through 4 mm nylon 0.2 μm filter to give a clear solution. LC-MS/MS analysis was performed using positive electrospray ionization (ESI+) source in multi-reaction-monitoring mode on a QTRAP 6500+ mass spectrometer from Sciex (Washington, USA), equipped with an Eksgience HALO ES peptide C18 column (50 mm × 0.5 mm, 2.7 μm). Solvent flow rate was set to 15 μL min^{-1}, and column temperature was kept at 50 °C. Injection volume was 5 μL. Mobile phase was 0.10% formic acid/water (A) and 0.10% formic acid/acetonitrile (B), with an elution gradient starting with 5% of eluent B, increasing to 100% in 4 min, and then back to initial conditions in 2 min for a total run time of 8 min. Optimized parameters were obtained by direct infusion of Pyr-apelin-13, **13**, and **15** analytical standard solutions at 100 ng mL^{-1} as follows: CUR, 20, CAD, medium, IS 5100 V, TEM, 300 °C, GS1, 15, and GS2 13. Two daughter traces (transitions) were used. The most abundant transition was used for quantification, the second most abundant for confirmation. Pyr-apelin-13, **13**, and **15** in the supernatant were analyzed after sample purification. Results are reported in the Supporting Information.

■ ASSOCIATED CONTENT

Supporting Information

The Supporting Information is available free of charge on the ACS Publications website at DOI: 10.1021/acs.jmedchem.7b01353.

Synthetic scheme of N_α-linked macrocyclic analogues and C-terminally modified macrocyclic, HRMS spectra and analytical UPLC-MS spectra, structure, molecular formula strings, half-life, and degradation profile in rat plasma of compounds, in vivo pharmacokinetic analysis of apelin-13, compounds **13** and **15**, binding curves of apelin-13, and compounds **13** and **15** on the rat apelin receptor (PDF)

Molecular formula strings (CSV)

■ AUTHOR INFORMATION

Corresponding Author

*Phone: +1 (819)821-8000 ext 72433. Fax: +1 (819)564-5400. E-mail: eric.marsault@usherbrooke.ca.

ORCID

Lounès Haroune: 0000-0001-5420-6619

Éric Marsault: 0000-0002-5305-8762

Author Contributions

⊥E.M. and P.S. contributed equally to directing this study.

Notes

The authors declare no competing financial interest.

■ ACKNOWLEDGMENTS

Financial support from Université de Sherbrooke, the Canadian Institutes of Health Research, the Natural Sciences and Engineering Research Council of Canada, Canada Foundation for Innovation and Merck Sharpe & Dohme (donation to the Faculty of Medicine and Health Sciences of Université de Sherbrooke) is gratefully acknowledged. The Canadian Francophonie Scholarship Program (PCBF), MITACS, and FRQS are also acknowledged for scholarship grants to K.T., A.M., X.S., and D.C., respectively. M.A.-M. is the recipient of a Heart and Stroke Foundation of Canada (HFSC) New Investigator award and a research scholar from the Fonds de la Recherche du Québec en Santé (FRQS). P.S. is the recipient of the Canada Research Chair in Neurophysiopharmacology of Chronic Pain. E.M. is a member of the FRQNT-funded Proteo Network and the FRQS-funded Réseau Québécois de Recherche sur le Médicament. We also thank Prof. Michel Bouvier (Institut de Recherche en Immunologie et Cancer, Montréal, Québec, Canada) for the use of human $G\alpha_{i1}$ and β-arrestin2 biosensors.

■ ABBREVIATIONS USED

AUC, area under curve; BRET, bioluminescence resonance energy transfer; DCM, dichloromethane; DIAD, diisopropylazodicarboxylate; DIPEA, *N*,*N*-diisopropylethylamine; DMF, *N*,*N*-dimethylformamide; GPCR, G protein-coupled receptor; HATU, *O*-(7-azabenzotriazol-1-yl)-1,1,3,3-tetramethyluronium hexafluorophosphate; HEK, human embryonic kidney; UPLC, ultra high performance liquid chromatography; HRMS, high resolution mass spectrometry; iPrOH, 2-propanol; LVDP, left ventricular developed pressure; MABP, mean arterial blood pressure; SAR, structure−activity relationship; TBME, *tert*-butyl methyl ether; TFA, trifluoroacetic acid; TIPS, triisopropylsilane

■ REFERENCES

(1) O'Dowd, B. F.; Heiber, M.; Chan, A.; Heng, H. H. Q.; Tsui, L.-C.; Kennedy, J. L.; Shi, X.; Petronis, A.; George, S. R.; Nguyen, T. A Human Gene That Shows Identity with the Gene Encoding the Angiotensin Receptor Is Located on Chromosome 11. *Gene* **1993**, *136*, 355−360.

(2) Tatemoto, K.; Hosoya, M.; Habata, Y.; Fujii, R.; Kakegawa, T.; Zou, M.-X.; Kawamata, Y.; Fukusumi, S.; Hinuma, S.; Kitada, C.; Kurokawa, T.; Onda, H.; Fujino, M. Isolation and Characterization of a Novel Endogenous Peptide Ligand for the Human APJ Receptor. *Biochem. Biophys. Res. Commun.* **1998**, *251*, 471−476.

(3) Wang, G.; Qi, X.; Wei, W.; Englander, E. W.; Greeley, G. H. Characterization of the 5′-Regulatory Regions of the Rat and Human Apelin Genes and Regulation of Breast Apelin by USF. *FASEB J.* **2006**, *20*, 2639−2641.

(4) Shin, K.; Pandey, A.; Liu, X.-Q.; Anini, Y.; Rainey, J. K. Preferential Apelin-13 Production by the Proprotein Convertase PCSK3 Is Implicated in Obesity. *FEBS Open Bio* **2013**, *3*, 328−333.

(5) Yang, P.; Kuc, R. E.; Brame, A. L.; Dyson, A.; Singer, M.; Glen, R. C.; Cheriyan, J.; Wilkinson, I. B.; Davenport, A. P.; Maguire, J. J. [Pyr1]Apelin-13(1−12) Is a Biologically Active ACE2Metabolite of the Endogenous Cardiovascular Peptide [Pyr1]Apelin-13. *Front. Neurosci.* **2017**, *11*, 92.

(6) Zhen, E. Y.; Higgs, R. E.; Gutierrez, J. A. Pyroglutamyl Apelin-13 Identified as the Major Apelin Isoform in Human Plasma. *Anal. Biochem.* **2013**, *442*, 1−9.

(7) Medhurst, A. D.; Jennings, C. A.; Robbins, M. J.; Davis, R. P.; Ellis, C.; Winborn, K. Y.; Lawrie, K. W. M.; Hervieu, G.; Riley, G.; Bolaky, J. E.; Herrity, N. C.; Murdock, P.; Darker, J. G. Pharmacological and Immunohistochemical Characterization of the APJ Receptor and Its Endogenous Ligand Apelin. *J. Neurochem.* **2003**, *84*, 1162−1172.

DOI: 10.1021/acs.jmedchem.7b01353
J. Med. Chem. 2018, 61, 2266−2277

(8) Messari, S. E.; Iturrioz, X.; Fassot, C.; De Mota, N.; Roesch, D.; Llorens-Cortes, C. Functional Dissociation of Apelin Receptor Signaling and Endocytosis: Implications for the Effects of Apelin on Arterial Blood Pressure. *J. Neurochem.* **2004**, *90*, 1290−1301.
(9) Narayanan, S.; Harris, D. L.; Maitra, R.; Runyon, S. P. Regulation of the Apelinergic System and Its Potential in Cardiovascular Disease: Peptides and Small Molecules as Tools for Discovery: Miniperspective. *J. Med. Chem.* **2015**, *58*, 7913−7927.
(10) Szokodi, I.; Tavi, P.; Földes, G.; Voutilainen-Myllylä, S.; Ilves, M.; Tokola, H.; Pikkarainen, S.; Piuhola, J.; Rysä, J.; Tóth, M.; Ruskoaho, H. Apelin, the Novel Endogenous Ligand of the Orphan Receptor APJ, Regulates Cardiac Contractility. *Circ. Res.* **2002**, *91*, 434−440.
(11) Perjés, Á.; Skoumal, R.; Tenhunen, O.; Kónyi, A.; Simon, M.; Horváth, I. G.; Kerkelä, R.; Ruskoaho, H.; Szokodi, I. Apelin Increases Cardiac Contractility via Protein Kinase Cε- and Extracellular Signal-Regulated Kinase-Dependent Mechanisms. *PLoS One* **2014**, *9*, e93473.
(12) Hashimoto, T.; Kihara, M.; Ishida, J.; Imai, N.; Yoshida, S.; Toya, Y.; Fukamizu, A.; Kitamura, H.; Umemura, S. Apelin Stimulates Myosin Light Chain Phosphorylation in Vascular Smooth Muscle Cells. *Arterioscler., Thromb., Vasc. Biol.* **2006**, *26*, 1267−1272.
(13) Dray, C.; Knauf, C.; Daviaud, D.; Waget, A.; Boucher, J.; Buléon, M.; Cani, P. D.; Attané, C.; Guigné, C.; Carpéné, C.; Burcelin, R.; Castan-Laurell, I.; Valet, P. Apelin Stimulates Glucose Utilization in Normal and Obese Insulin-Resistant Mice. *Cell Metab.* **2008**, *8*, 437−445.
(14) Kim, J. Apelin-APJ Signaling: A Potential Therapeutic Target for Pulmonary Arterial Hypertension. *Mol. Cells* **2014**, *37*, 196−201.
(15) Kang, Y.; Kim, J.; Anderson, J. P.; Wu, J.; Gleim, S. R.; Kundu, R. K.; McLean, D. L.; Kim, J.; Park, H.; Jin, S.; Hwa, J.; Quertermous, T.; Chun, H. J. Apelin-APJ Signaling Is a Critical Regulator of Endothelial MEF2 Activation in Cardiovascular Development. *Circ. Res.* **2013**, *113*, 22−31.
(16) Masri, B.; Morin, N.; Cornu, M.; Knibiehler, B.; Audigier, Y. Apelin (65−77) Activates p70 S6 Kinase and Is Mitogenic for Umbilical Endothelial Cells. *FASEB J.* **2004**, *18*, 1909−1911.
(17) Masri, B.; Morin, N.; Pedebernade, L.; Knibiehler, B.; Audigier, Y. The Apelin Receptor Is Coupled to Gi1 or Gi2 Protein and Is Differentially Desensitized by Apelin Fragments. *J. Biol. Chem.* **2006**, *281*, 18317−18326.
(18) Chng, S. C.; Ho, L.; Tian, J.; Reversade, B. ELABELA: A Hormone Essential for Heart Development Signals via the Apelin Receptor. *Dev. Cell* **2013**, *27*, 672−680.
(19) Pauli, A.; Norris, M. L.; Valen, E.; Chew, G.-L.; Gagnon, J. A.; Zimmerman, S.; Mitchell, A.; Ma, J.; Dubrulle, J.; Reyon, D.; Tsai, S. Q.; Joung, J. K.; Saghatelian, A.; Schier, A. F. Toddler: An Embryonic Signal That Promotes Cell Movement via Apelin Receptors. *Science* **2014**, *343*, 1248636.
(20) Murza, A.; Sainsily, X.; Coquerel, D.; Côté, J.; Marx, P.; Besserer-Offroy, É.; Longpré, J.-M.; Lainé, J.; Reversade, B.; Salvail, D.; Leduc, R.; Dumaine, R.; Lesur, O.; Auger-Messier, M.; Sarret, P.; Marsault, É. Discovery and Structure−Activity Relationship of a Bioactive Fragment of ELABELA That Modulates Vascular and Cardiac Functions. *J. Med. Chem.* **2016**, *59*, 2962−2972.
(21) Kidoya, H.; Naito, H.; Muramatsu, F.; Yamakawa, D.; Jia, W.; Ikawa, M.; Sonobe, T.; Tsuchimochi, H.; Shirai, M.; Adams, R. H.; Fukamizu, A.; Takakura, N. APJ Regulates Parallel Alignment of Arteries and Veins in the Skin. *Dev. Cell* **2015**, *33*, 247−259.
(22) Kim, J.-D.; Kang, Y.; Kim, J.; Papangeli, I.; Kang, H.; Wu, J.; Park, H.; Nadelmann, E.; Rockson, S. G.; Chun, H. J.; Jin, S.-W. Essential Role of Apelin Signaling During Lymphatic Development in Zebrafish. *Arterioscler., Thromb., Vasc. Biol.* **2014**, *34*, 338−345.
(23) Yang, P.; Maguire, J. J.; Davenport, A. P. Apelin, Elabela/Toddler, and Biased Agonists as Novel Therapeutic Agents in the Cardiovascular System. *Trends Pharmacol. Sci.* **2015**, *36*, 560−567.
(24) Chamberland, C.; Barajas-Martinez, H.; Haufe, V.; Fecteau, M.-H.; Delabre, J.-F.; Burashnikov, A.; Antzelevitch, C.; Lesur, O.; Chraibi, A.; Sarret, P.; Dumaine, R. Modulation of Canine Cardiac Sodium Current by Apelin. *J. Mol. Cell. Cardiol.* **2010**, *48*, 694−701.
(25) Pitkin, S. L.; Maguire, J. J.; Kuc, R. E.; Davenport, A. P. Modulation of the Apelin/APJ System in Heart Failure and Atherosclerosis in Man. *Br. J. Pharmacol.* **2010**, *160*, 1785−1795.
(26) Folino, A.; Montarolo, P. G.; Samaja, M.; Rastaldo, R. Effects of Apelin on the Cardiovascular System. *Heart Failure Rev.* **2015**, *20*, 505−518.
(27) Japp, A. G.; Cruden, N. L.; Amer, D. A. B.; Li, V. K. Y.; Goudie, E. B.; Johnston, N. R.; Sharma, S.; Neilson, I.; Webb, D. J.; Megson, I. L.; Flapan, A. D.; Newby, D. E. Vascular Effects of Apelin In Vivo in Man. *J. Am. Coll. Cardiol.* **2008**, *52*, 908−913.
(28) Japp, A. G.; Cruden, N. L.; Barnes, G.; van Gemeren, N.; Mathews, J.; Adamson, J.; Johnston, N. R.; Denvir, M. A.; Megson, I. L.; Flapan, A. D.; Newby, D. E. Acute Cardiovascular Effects of Apelin in Humans: Potential Role in Patients with Chronic Heart Failure. *Circulation* **2010**, *121*, 1818−1827.
(29) Brash, L.; Barnes, G.; Brewis, M.; Church, C.; Gibbs, S.; Howard, L.; Johnson, M.; McGlinchey, N.; Simpson, J.; Stirrat, C.; Thomson, S.; Watson, G.; Welsh, D.; Wilkins, M.; Newby, D.; Peacock, A. Apelin Improves Cardiac Output in Patients with Pulmonary Arterial Hypertension. *Eur. Respir. J.* **2015**, *46*, PA2107.
(30) Berry, M. F.; Pirolli, T. J.; Jayasankar, V.; Burdick, J.; Morine, K. J.; Gardner, T. J.; Woo, Y. J. Apelin Has In Vivo Inotropic Effects on Normal and Failing Hearts. *Circulation* **2004**, *110*, II-187−II-193.
(31) Read, C.; Fitzpatrick, C. M.; Yang, P.; Kuc, R. E.; Maguire, J. J.; Glen, R. C.; Foster, R. E.; Davenport, A. P. Cardiac Action of the First G Protein Biased Small Molecule Apelin Agonist. *Biochem. Pharmacol.* **2016**, *116*, 63−72.
(32) Yang, P.; Read, C.; Kuc, R. E.; Buonincontri, G.; Southwood, M.; Torella, R.; Upton, P. D.; Crosby, A.; Sawiak, S. J.; Carpenter, T. A.; Glen, R. C.; Morrell, N. W.; Maguire, J. J.; Davenport, A. P. Elabela/Toddler Is an Endogenous Agonist of the Apelin APJ Receptor in the Adult Cardiovascular System, and Exogenous Administration of the Peptide Compensates for the Downregulation of Its Expression in Pulmonary Arterial Hypertension. *Circulation* **2017**, *135*, 1160−1173.
(33) Chagnon, F.; Coquerel, D.; Salvail, D.; Marsault, E.; Dumaine, R.; Auger-Messier, M.; Sarret, P.; Lesur, O. M. Apelin Compared With Dobutamine Exerts Cardioprotection and Extends Survival in a Rat Model of Endotoxin-Induced Myocardial Dysfunction. *Crit. Care Med.* **2017**, *45*, e391−e398.
(34) Coquerel, D.; Chagnon, F.; Sainsily, X.; Dumont, L.; Murza, A.; Côté, J.; Dumaine, R.; Sarret, P.; Marsault, É.; Salvail, D.; Auger-messier, M.; Lesur, O. Elabela Improves Cardio-Renal Outcome in Fatal Experimental Septic Shock. *Crit. Care Med.* **2017**, *45*, e1139−e1148.
(35) Vickers, C.; Hales, P.; Kaushik, V.; Dick, L.; Gavin, J.; Tang, J.; Godbout, K.; Parsons, T.; Baronas, E.; Hsieh, F.; Acton, S.; Patane, M.; Nichols, A.; Tummino, P. Hydrolysis of Biological Peptides by Human Angiotensin-Converting Enzyme-Related Carboxypeptidase. *J. Biol. Chem.* **2002**, *277*, 14838−14843.
(36) Murza, A.; Belleville, K.; Longpré, J.-M.; Sarret, P.; Marsault, É. Stability and Degradation Patterns of Chemically Modified Analogs of Apelin-13 in Plasma and Cerebrospinal Fluid. *Biopolymers* **2014**, *102*, 297−303.
(37) McKinnie, S. M. K.; Fischer, C.; Tran, K. M. H.; Wang, W.; Mosquera, F.; Oudit, G. Y.; Vederas, J. C. The Metalloprotease Neprilysin Degrades and Inactivates Apelin Peptides. *ChemBioChem* **2016**, *17*, 1495−1498.
(38) Gerbier, R.; Alvear-Perez, R.; Margathe, J.-F.; Flahault, A.; Couvineau, P.; Gao, J.; De Mota, N.; Dabire, H.; Li, B.; Ceraudo, E.; Hus-Citharel, A.; Esteoulle, L.; Bisoo, C.; Hibert, M.; Berdeaux, A.; Iturrioz, X.; Bonnet, D.; Llorens-Cortes, C. Development of Original Metabolically-Stable Apelin-17 Analogs with Diuretic and Cardiovascular Effects. *FASEB J.* **2017**, *31*, 687−700.
(39) Juhl, C.; Els-Heindl, S.; Schönauer, R.; Redlich, G.; Haaf, E.; Wunder, F.; Riedl, B.; Burkhardt, N.; Beck-Sickinger, A. G.; Bierer, D. Development of Potent and Metabolically Stable APJ Ligands with High Therapeutic Potential. *ChemMedChem* **2016**, *11*, 2378−2384.

DOI: 10.1021/acs.jmedchem.7b01353
J. Med. Chem. 2018, 61, 2266−2277

(40) McKinnie, S. M. K.; Wang, W.; Fischer, C.; McDonald, T.; Kalin, K. R.; Iturrioz, X.; Llorens-Cortes, C.; Oudit, G. Y.; Vederas, J. C. Synthetic Modification within the "RPRL" Region of Apelin Peptides: Impact on Cardiovascular Activity and Stability to Neprilysin and Plasma Degradation. *J. Med. Chem.* **2017**, *60*, 6408−6427.
(41) Marsault, E.; Peterson, M. L. Macrocycles are Great Cycles: Applications, Opportunities, and Challenges of Synthetic Macrocycles in Drug Discovery. *J. Med. Chem.* **2011**, *54*, 1961−2004.
(42) Marsault, E., Peterson, M. L. *Practical Medicinal Chemistry with Macrocycles: Design, Synthesis, and Case Studies*; Wiley: Hoboken, NJ, 2017.
(43) Zecri, F.; Golosov, A.; Grosche, P.; DK; Zhao, H.; Hu, Q.-Y.; Imase, H. Synthetic Apelin Mimetics for the Treatment of Heart Failure. U. S. Patent 9067971, June 30, 2015.
(44) Brame, A. L.; Maguire, J. J.; Yang, P.; Dyson, A.; Torella, R.; Cheriyan, J.; Singer, M.; Glen, R. C.; Wilkinson, I. B.; Davenport, A. P. Design, Characterization, and First-In-Human Study of the Vascular Actions of a Novel Biased Apelin Receptor Agonist. *Hypertension* **2015**, *65*, 834−840.
(45) Macaluso, N. J. M.; Pitkin, S. L.; Maguire, J. J.; Davenport, A. P.; Glen, R. C. Discovery of a Competitive Apelin Receptor (APJ) Antagonist. *ChemMedChem* **2011**, *6*, 1017−1023.
(46) Murza, A.; Sainsily, X.; Côté, J.; Bruneau-Cossette, L.; Besserer-Offroy, É.; Longpré, J.-M.; Leduc, R.; Dumaine, R.; Lesur, O.; Auger-Messier, M.; Sarret, P.; Marsault, É. Structure−activity Relationship of Novel Macrocyclic Biased Apelin Receptor Agonists. *Org. Biomol. Chem.* **2017**, *15*, 449−458.
(47) Ma, Y.; Yue, Y.; Ma, Y.; Zhang, Q.; Zhou, Q.; Song, Y.; Shen, Y.; Li, X.; Ma, X.; Li, C.; Hanson, M. A.; Han, G. W.; Sickmier, E. A.; Swaminath, G.; Zhao, S.; Stevens, R. C.; Hu, L. A.; Zhong, W.; Zhang, M.; Xu, F. Structural Basis for Apelin Control of the Human Apelin Receptor. *Structure* **2017**, *25*, 858−866 e4..
(48) Reichwein, J. F.; Wels, B.; Kruijtzer, J. A. W.; Versluis, C.; Liskamp, R. M. J. Rolling Loop Scan: An Approach Featuring Ring-Closing Metathesis for Generating Libraries of Peptides with Molecular Shapes Mimicking Bioactive Conformations or Local Folding of Peptides and Proteins. *Angew. Chem., Int. Ed.* **1999**, *38*, 3684−3687.
(49) Murza, A.; Parent, A.; Besserer-Offroy, E.; Tremblay, H.; Karadereye, F.; Beaudet, N.; Leduc, R.; Sarret, P.; Marsault, É. Elucidation of the Structure-Activity Relationships of Apelin: Influence of Unnatural Amino Acids on Binding, Signaling, and Plasma Stability. *ChemMedChem* **2012**, *7*, 318−325.
(50) Kan, T.; Fukuyama, T. Ns Strategies: A Highly Versatile Synthetic Method for Amines. *Chem. Commun.* **2004**, *0* (4), 353−359.
(51) Chatterjee, J.; Laufer, B.; Kessler, H. Synthesis of N-Methylated Cyclic Peptides. *Nat. Protoc.* **2012**, *7* (3), 432−444.
(52) Carpino, L. A.; Han, G. Y. 9-Fluorenylmethoxycarbonyl Amino-Protecting Group. *J. Org. Chem.* **1972**, *37* (22), 3404−3409.
(53) Murza, A.; Besserer-Offroy, É.; Côté, J.; Bérubé, P.; Longpré, J.-M.; Dumaine, R.; Lesur, O.; Auger-Messier, M.; Leduc, R.; Sarret, P.; Marsault, É. C-Terminal Modifications of Apelin-13 Significantly Change Ligand Binding, Receptor Signaling, and Hypotensive Action. *J. Med. Chem.* **2015**, *58*, 2431−2440.
(54) Patgiri, A.; Menzenski, M. Z.; Mahon, A. B.; Arora, P. S. Solid-Phase Synthesis of Short α-Helices Stabilized by the Hydrogen Bond Surrogate Approach. *Nat. Protoc.* **2010**, *5*, 1857−1865.
(55) Lee, D. K.; Ferguson, S. S. G.; George, S. R.; O'Dowd, B. F. The Fate of the Internalized Apelin Receptor Is Determined by Different Isoforms of Apelin Mediating Differential Interaction with β-Arrestin. *Biochem. Biophys. Res. Commun.* **2010**, *395*, 185−189.
(56) Macaluso, N. J. M.; Glen, R. C. Exploring the "RPRL" Motif of Apelin-13 through Molecular Simulation and Biological Evaluation of Cyclic Peptide Analogues. *ChemMedChem* **2010**, *5*, 1247−1253.
(57) Langelaan, D. N.; Bebbington, E. M.; Reddy, T.; Rainey, J. K. Structural Insight into G-Protein Coupled Receptor Binding by Apelin. *Biochemistry* **2009**, *48*, 537−548.
(58) Ruiz-Gómez, G.; Tyndall, J. D. A.; Pfeiffer, B.; Abbenante, G.; Fairlie, D. P. Update 1 of: Over One Hundred Peptide-Activated G Protein-Coupled Receptors Recognize Ligands with Turn Structure. *Chem. Rev.* **2010**, *110*, PR1−PR41.
(59) Lee, D. K.; Saldivia, V. R.; Nguyen, T.; Cheng, R.; George, S. R.; O'Dowd, B. F. Modification of the Terminal Residue of Apelin-13 Antagonizes Its Hypotensive Action. *Endocrinology* **2005**, *146*, 231−236.
(60) Pilowsky, P. M.; Goodchild, A. K. Baroreceptor Reflex Pathways and Neurotransmitters: 10 Years on. *J. Hypertens.* **2002**, *20*, 1675−1688.
(61) Langendorff, O. Untersuchungen am Überlebenden Säugethier-herzen. *Pfluegers Arch.* **1895**, *61*, 291−332.
(62) Yung-Chi, C.; Prusoff, W. H. Relationship between the Inhibition Constant (KI) and the Concentration of Inhibitor Which Causes 50 per Cent Inhibition (I50) of an Enzymatic Reaction. *Biochem. Pharmacol.* **1973**, *22*, 3099−3108.
(63) Zimmerman, B.; Beautrait, A.; Aguila, B.; Charles, R.; Escher, E.; Claing, A.; Bouvier, M.; Laporte, S. A. Differential β-Arrestin−Dependent Conformational Signaling and Cellular Responses Revealed by Angiotensin Analogs. *Sci. Signaling* **2012**, *5*, ra33−ra33.
(64) Galés, C.; Van Durm, J. J. J.; Schaak, S.; Pontier, S.; Percherancier, Y.; Audet, M.; Paris, H.; Bouvier, M. Probing the Activation-Promoted Structural Rearrangements in Preassembled receptor−G Protein Complexes. *Nat. Struct. Mol. Biol.* **2006**, *13*, 778−786.

DOI: 10.1021/acs.jmedchem.7b01353
J. Med. Chem. 2018, 61, 2266−2277